be small, since the pyridine is coordinated trans to a CO_2^- group in both cases. Structurally these two sites are not equivalent. It has been noted before that polydentate ligands such as $^-O_2C-CH_2-NH-CH_2-CO_2^-$, $IMDA^{2-}$, can coordinate in two ways.[21,29,35] In the facial mode, the glycinate chelate rings are 90° to each other, and there is very little strain in the C–N–C angle. In the meridional mode the glycinate chelate rings are in the same plane. This type of coordination causes considerable strain in the C–N–C angle. Thus coordination of the pyridine trans to the β-CO_2^- group in Co(PLASP)(L-Phe) likewise gives the least strain at N1 and allows the rigid chelate ring Co–N1–C5–C6–N2 (along with the entire pyridine ring) to be planar.

If the coordination of the phenylalaninate ligand is considered next, there are two ways it can coordinate as shown in Figure 1a,c. Coordination as in Figure 1a would be electronically favored since the amino group is trans to oxygen (the carboxylate group). It has been noted before,[6,37,38] that amino groups avoid coordinating trans to each other, which would favor the structure in Figure 1a over that in Figure 1c. Additional support for facial coordination is given in an earlier theoretical account of bonding in transition-metal complexes which states that the most stable isomer for low-spin d^6 $ML_3L'3$ complexes should be facial.[39] This appears to be the case in complexes where no steric interaction is evident. Also, coordination as in Figure 1a is sterically favored since the α-carbon of the phenylalaninate chelate ring is pointing up and away from the pyridine ring. This configuration of the L-Phe^- ring is determined by the bulky R group, $-CH_2-Ph$, which would favor the equatorial rather than axial position.

Acknowledgment. The authors thank J. H. Benson and B. J. Helland for their assistance in collecting the X-ray data. We thank the National Institute of General Medical Sciences for primary support of this research through Grant GM12626. Partial support was provided by the U.S. Department of Energy, Office of Basic Energy Sciences, Material Sciences Division.

Registry No. [Co(PLASP)(L-Phe)]·$3H_2O$, 73396-77-7; $PLASPH_2$, 41203-01-4; L-aspartic acid, 56-84-8; 2-pyridinecarboxaldehyde, 1121-60-4.

Supplementary Material Available: A table listing observed and calculated structure factors (5 pages). Ordering information is given on any current masthead page.

---

[37] Watabe, M.; Zama, M.; Yoshikawa, S. *Bull. Chem. Soc. Jpn.* **1978**, *51*, 1354.

[38] Ebner, S. R.; Angelici, R. J., unpublished results.

[39] Burdett, J. K. *Adv. Inorg. Chem. Radiochem.* **1978**, *21*, 113.

Contribution from the Department of Chemistry,
University of California, Berkeley, California 94720

Coordination Chemistry of Microbial Iron Transport Compounds. 20. Crystal and Molecular Structures of Two Salts of *cis*- and *trans*-Tris(benzohydroximato)chromate(III)[1]

KAMAL ABU-DARI[2] and KENNETH N. RAYMOND*

Received September 26, 1979

The isolation of crystalline solids of *cis*- and *trans*-tris(benzohydroximato)chromate(III) salts is reported. The structures of both isomers have been determined by single-crystal X-ray diffraction, using automated counter data. Interisomerization of the neutral hydroxamato and anionic hydroximato complexes occurs via loss of a proton on the hydroxamate nitrogens. This deprotonation results in only small changes in the geometry of either the CrO_6 coordination polyhedron or the ligand. These results support a view of these complexes as rigid, octahedral complexes in which the hydroxamate ligand has substantial negative charge on both oxygen atoms and nearly full formation of a C═N double bond in the center of the ring. The Cr–O bond lengths average 1.955 (13) and 1.987 (12) Å for the *N*-hydroxyl and carbonyl oxygens in the trans isomers, while the corresponding distances in the cis isomer are 1.951 (4) and 1.965 (2) Å. The structures of the *cis*- and *trans*-tris(benzohydroximato)chromate(III) complexes were solved by direct phasing methods followed by full-matrix least-squares and Fourier techniques. Green-purple crystals of the cis isomer conform to space group $P\bar{3}c1$ with a = 13.762 (1) Å, c = 26.238 (2) Å, V = 4304 (2) Å^3, Z = 4, ρ_{calcd} = 1.58 g cm^{-3}, and ρ_{obsd} = 1.57 g cm^{-3}. Refinement using 2612 reflections with $F^2 > 3\sigma(F^2)$ gave R = 4.39% and R_w = 6.45%. Green–purple crystals of the trans isomer conform to space group $P2_1/n$ with a = 10.310 (3) Å, b = 11.208 (2) Å, c = 28.638 (5) Å, β = 93.65 (2)°, V = 3203 (2) Å^3, Z = 4, ρ_{calcd} = 1.44 g cm^{-3}, and ρ_{obsd} = 1.42 g cm^{-3}. Refinement using 4617 reflections with $F^2 > 3\sigma(F^2)$ gave R = 3.89% and R_w = 4.61%.

Introduction

The siderophores are low-molecular-weight compounds whose manufacture by microbes, in order to facilitate the uptake of ferric iron, we have described in previous papers in this series[1] and in recent reviews.[3] The most common functional groups in the siderophores are the hydroxamate group as in ferrichromes[4] and ferrioxamines[5] and the catecholate group as in enterobactin.[6] Replacing the ferric ion (high-spin d^5 system) by the chromic ion (d^3) produces inert complexes which may be used as chemical probes in studying the iron-transport mechanism in living systems.[7,8] Unlike the ferric

---

[1] Part 19: Harris, W. R; Carrano, C. J.; Cooper, S. R.; Sofen, S. R.; Avdeef, A.; McArdle, J. V.; Raymond, K. N. *J. Am. Chem. Soc.* **1979**, *101*, 6097–104.

[2] US-AID Fellow.

[3] (a) Raymond, K. N. *Adv. Chem. Ser.* **1977**, *No. 162*, 33–54. (b) Raymond, K. N.; Carrano, C. J. *Acc. Chem. Res.* **1979**, *12*, 183–90. (c) Raymond, K. N.; Abu-Dari, K.; Sofen, S. R. *ACS Symp. Ser.*, in press.

[4] Leong, J.; Raymond, K. N. *J. Am. Chem. Soc.* **1974**, *96*, 6628–30.

[5] Leong, J.; Raymond, K. N. *J. Am. Chem. Soc.* **1975**, *97*, 293–6.

[6] Isied, S. S.; Kuo, G.; Raymond, K. N. *J. Am. Chem. Soc.* **1976**, *98*, 1763–7.

[7] Leong, J.; Neilands, J. B.; Raymond, K. N. *Biochem. Biophys. Res. Commun.* **1974**, *60*, 1066–71.

[8] Carrano, C. J.; Raymond, K. N. *J. Bacteriol.* **1978**, *136*, 69–74.

0020-1669/80/1319-2034$01.00/0 © 1980 American Chemical Society

siderophore complexes, of which only the cis geometrical isomers have been characterized, both the cis and trans geometrical isomers of the chromic complexes of deferriferrioxamine B[5] and rhodotorulic acid[9,10] as well as simple hydroxamates[11] have been separated and characterized in solution. We recently reported the structural characterization of *trans*-tris(benzohydroxamato)chromium(III);[12] however, we were unable to crystallize the cis isomer due to its instability in most solutions.

Deprotonation of N-unsubstituted tris(hydroxamato)metal complexes in strongly basic solution results in the formation of tris(hydroximato)metal anionic complexes:

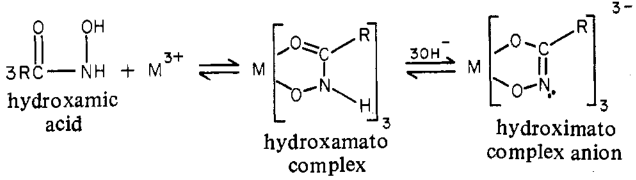

This is a reaction we previously used to resolve metal complexes by first resolving the anionic hydroximato complex with the optical isomers of $[Co(en)_3]^{3+}$, followed by protonation and isolation of the resolved hydroxamato complexes.[13]

Recently we reported the isolation and structural characterization of a tris(thiobenzohydroximato)chromate(III) salt,[14] and its structure was compared with that of the corresponding thiohydroxamato complex.[15] In this paper we report the isolation and characterization of both the *cis*- and the *trans*-tris(benzohydroximato)chromate(III) anions, including the X-ray structural determination of the salts of both complexes. The structures of the hydroximato complexes will be compared with that of *trans*-tris(benzohydroxamato)chromium(III), with attention particularly focused on (1) the changes that occur in ligand bonding upon conversion of the hydroxamate $[RC(O)—N(O)H]^-$ to the hydroximate $[RC(O)=N(O)]^{2-}$ anions and (2) comparison of the coordination geometries of both the *cis*- and *trans*-tris(hydroximato)chromate(III) isomers with that of the neutral hydroxamato complex.

Experimental Section

Materials. Analytical grade solvents and chemicals were used throughout; *cis*- and *trans*-tris(benzohydroxamato)chromium(III) were prepared as described in a previous paper of this series.[12]

Microanalysis. Microanalyses were performed by the Microanalytical Laboratory, Department of Chemistry, University of California at Berkeley.

***cis*-Tris(benzohydroximato)chromate(III) Salt.** *trans*-Tris(benzohydroxamato)chromium(III) (4.57 g, 10 mmol) was dissolved in a degassed aqueous solution of sodium hydroxide (60 mL, 2.5 M). To this solution was added a solution of triethylmethylammonium iodide (15 g) in 30 mL of water. The resulting solution was filtered and its volume reduced by low-pressure evaporation until the appearance of turbidity. The solution was then heated to ~80 °C, ethanol–methanol (1:1, 30 mL) was added, and the solution was left for several days for crystallization. The crystals, dichroic green–purple hexagonal rods, were filtered, washed with a small amount of cold water, and dried in air at room temperature. Anal. Calcd for $Na_3Cr(C_7H_5NO_2)_3{\cdot}NaI{\cdot}NaOH{\cdot}9H_2O{\cdot}3CH_3OH{\cdot}C_2H_5OH$: C, 30.60; H, 5.14; N, 4.12; Na, 11.26. Found: C, 30.14; H, 4.81; N, 4.18; Na, 10.8. Absorption spectrum (in 2.5 M NaOH solution), λ_{max} nm (ϵ): 579 (92.0), 415 (143).

Table I. Summary of Crystal Data for *cis*- and *trans*-$[Cr(benz\text{-}H)_3]^{3-}$ Complexes

	$Na_3Cr(benz\text{-}H)_3{\cdot}NaI{\cdot}9H_2O{\cdot}3CH_3OH{\cdot}C_2H_5OH$	$Na_3Cr(benz\text{-}H)_3{\cdot}8H_2O{\cdot}C_2H_5OH$
mol wt	1020.6	716.4
space group	$P\bar{3}c1$	$P2_1/n$
cell const[a]		
a, Å	13.762 (1)	10.310 (3)
b, Å		11.208 (2)
c, Å	26.238 (3)	28.638 (5)
β, deg		93.65 (2)
cell vol, Å^3	4303 (2)	3203 (2)
formula units/cell	4	4
calcd density, g/cm^3	1.575	1.44
obsd density, g/cm^3	1.570 (5)	1.42 (1)
cryst dimens, mm	0.24 × 0.24 × 0.40	0.18 × 0.35 × 0.35
linear coeff, cm^{-1} ($\mu_{MoK\alpha}$)	11.4	4.78

[a] Ambient temperature of 23 °C; Mo $K\alpha_1$ radiation, λ = 0.709 26 Å.

***trans*-Tris(benzohydroximato)chromate(III) Salt.** *cis*-Tris(benzohydroxamato)chromium(III) (4.57 g, 10 mmol) was dissolved in a degassed aqueous solution of sodium hydroxide (60 mL, 2.5 M). The solution was filtered and the volume reduced by low-pressure evaporation until the appearance of turbidity. The solution was then heated to ~80 °C, ethanol (20 mL) was added, and the solution was left for 2 weeks for crystallization. The crystals, dichroic green–purple rectangular plates, were filtered, washed with a small amount of cold water, and dried in air at room temperature. Anal. Calcd for $Na_3Cr(C_7H_5NO_2)_3{\cdot}8H_2O{\cdot}C_2H_5OH$: C, 38.56; H, 5.20; N, 5.86; Na, 9.63. Found: C, 38.63; H, 5.01; N, 5.98; Na, 9.60. Absorption spectrum (in 2.5 M NaOH solution), λ_{max} nm (ϵ): 586 (88), 400 (sh, 137).

Unit Cell and Diffraction Data. Precession photographs for the *cis*-tris(benzohydroximato)chromate(III) (*cis*-$[Cr(benz\text{-}H)_3]^{3-}$) salt showed trigonal symmetry with the systematic absence of $\bar{h}0l$, $l = 2n$, reflections. Two space groups consistent with these conditions are $P3c1$ and $P\bar{3}c1$. Careful examination of the intensity data showed the presence of some of the $\bar{h}0l$, $l = 2n$, reflections. However, the final structure confirms the choice of space group as $P\bar{3}c1$. The weak violation of the *c* glide extinctions are most likely due to a small twin of the main single crystal. Laue symmetry $2/m$ was observed for *trans*-tris(benzohydroximato)chromate(III) (*trans*-$[Cr(benz\text{-}H)_3]^{3-}$) salt, with $h0l$, $h + l = 2n$, and $0k0$, $k = 2n$, defining the space group as $P2_1/n$ (an alternate setting of $P2_1/c$, No. 14). Unit cell data for both structures, obtained by a least-squares fit of 22 high-angle reflections for each, are given in Table I.

Intensity data were collected on an Enraf-Nonius CAD-4 automated diffractometer controlled by a PDP-8/E computer by using monochromatic Mo Kα radiation.[16,17] The data were reduced to F^2 and $\sigma(F^2)$ values as previously described[12,18] and averaged to give 2612

---

(9) Carrano, C. J.; Raymond, K. N. *J. Chem. Soc., Chem. Commun.* **1978**, 501–2.

(10) Carrano, C. J.; Raymond, K. N. *J. Am. Chem. Soc.* **1978**, *100*, 5371–4.

(11) Leong, J.; Raymond, K. N. *J. Am. Chem. Soc.* **1974**, *96*, 1757–62.

(12) Abu-Dari, K.; Ekstrand, J. D.; Freyberg, D. P.; Raymond, K. N. *Inorg. Chem.* **1979**, *18*, 108–12.

(13) Abu-Dari, K.; Raymond, K. N. *J. Am. Chem. Soc.* **1977**, *99*, 2003–5.

(14) Abu-Dari, K.; Freyberg, D. P.; Raymond, K. N. *Inorg. Chem.* **1979**, *18*, 2427–33.

(15) Freyberg, D. P.; Abu-Dari, K.; Raymond, K. N. *Inorg. Chem.* **1979**, *18*, 3037–43.

(16) The Enraf-Nonius Fortran IV system operates the CAD-4 diffractometer. In addition to locally written programs for the CDC-7600, the following programs or modifications were used: Zalkin's FORDAP Fourier program; Ibers' NUCLS, a group least-square version of the Busing–Levy ORFLS program; ORFFE, a function and error program by Busing and Levy; MULTAN, a program series for direct-method phase determination by Germain, Main, and Woolfson.

(17) The intensities of duplicate sets of reflections ($-h,k,l$) with 2° < 2θ < 60° for *cis*-$[Cr(benz\text{-}H)_3]^{3-}$ complex and unique sets of reflections ($h,k,\pm l$) with 2° < 2θ < 55° for *trans*-$[Cr(benz\text{-}H)_3]^{3-}$ isomer were measured by using a θ–2θ scan technique. The θ scan angle was calculated as 0.60 + 0.35 tan θ. An aperture with a height of 2 mm and variable width [width (mm) = 2.00 + 0.5 tan θ] was located 173 mm from the crystal. For each reflection the scan angle was extended 25% on either side to estimate the background count. The scan time was variable, with a maximum of 90 s. The intensities of three standard reflections were monitored regularly and showed no significant fluctuation. Three orientation standard reflections were monitored regularly and showed no change in setting angle greater than 0.1° in any axis. An attenuator to decrease the intensity of the diffracted beam by a factor of 18.17 was inserted into the beam when the prescan indicated an intensity too high for accurate counting (I > 50 000 counts/s).

(18) Baker, E. C.; Brown, L. D.; Raymond, K. N. *Inorg. Chem.* **1975**, *14*, 1376–9.

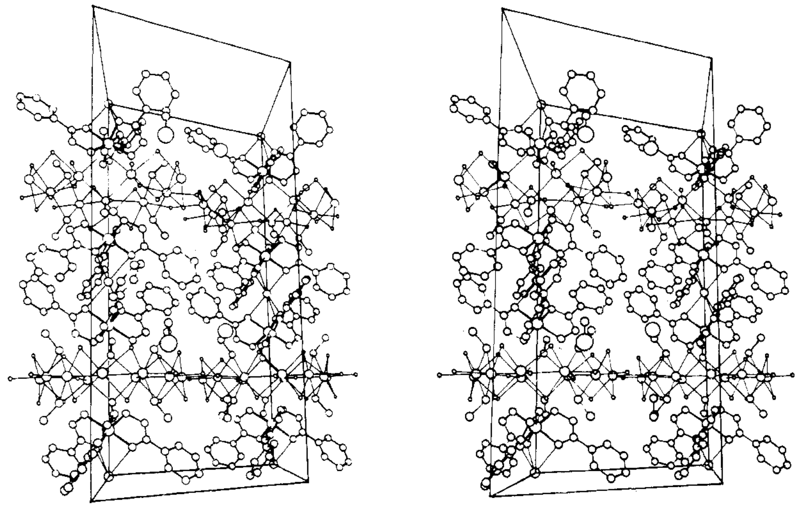

Figure 1. Stereoscopic packing diagrams of the compound *cis*-$Na_3[Cr(PhC(O){=}N(O))_3]\cdot NaI\cdot NaOH\cdot 9H_2O\cdot 3CH_3OH\cdot C_2H_5OH$. The structure is viewed down the crystallographic *a* axis. The vertical axis is *c*.

and 4617 independent data [with $F^2 > 3\sigma(F^2)$] and *R* factors for averaging of 2.5 and 1.1 for the cis and trans isomers, respectively. The parameter *p*, introduced to prevent overweighting of the strong reflections,[18] was set to 0.03. Lorentz and polarization corrections were applied. An absorption correction was applied for the cis isomer but was considered unnecessary for the trans isomer (μ = 4.78 cm^{-1}). The crystal densities were determined by the flotation technique in an iodobutane–heptane solution. The measured densities for both structures are given in Table I.

Solution and Refinement of Structures

cis-**[Cr(benz-H)$_3$]$^{3-}$ Salt.** The positions of the iodide and chromium atoms were obtained with MULTAN[16] using the 300 highest *E* values. This led to the location of all the nonhydrogen atoms by standard difference Fourier and least-squares techniques.[19-22] Examination of the Fourier map showed disorder in the position of the methyl group of the ethanol molecule about the threefold axis; the peaks found around this axis were refined with partial occupancy. After anisotropic refinement of the nonhydrogen atoms the positions of the phenyl hydrogens were calculated and were introduced as fixed atoms with B = 7.0 Å^2. The water hydrogens were located from the difference Fourier map and were introduced as fixed atoms with B = 5.0 Å^2. Full-matrix least-squares refinement with 174 variables, using the 2612 reflections with $F^2 > 3\sigma(F^2)$, led to convergence with R = 4.39%, R_w = 6.45%, and the error in an observation of unit weight = 2.47. The largest peaks in the final difference Fourier map were 0.41 and 0.27 e/Å^3, were located within 1 Å of the iodine and chromium atoms, respectively, and are most likely artifacts of a small twin of the crystal.

trans-**[Cr(benz-H)$_3$]$^{3-}$ Salt.** The positions of the chromium, sodium, and the hydroximate ring atoms were obtained with MULTAN[16] using the 300 highest *E* values. This led to the location of all the nonhydrogen atoms by standard difference Fourier and least-squares techniques.[19-22] The positions of the phenyl hydrogen atoms were calculated and found to match those found in the difference Fourier synthesis; these phenyl hydrogens were introduced along with water hydrogens and some ethanol hydrogens as fixed atoms in the final refinement with B = 5.0 Å^2. Full-matrix least-squares refinement with 407 variables, using the 4617 reflections with $F^2 > 3\sigma(F^2)$, led to convergence with R = 3.89%, R_w = 4.61%, and the error in an observation of unit weight = 1.63. The largest peaks in the final difference Fourier map were <0.17 e/Å^3.

Table II gives the positions and thermal parameters of the nonhydrogen atoms, and Tables IIIa[23] and IIIb[23] give the root-mean-squares amplitudes of vibration for the nonhydrogen atoms for the cis and trans isomers, respectively.

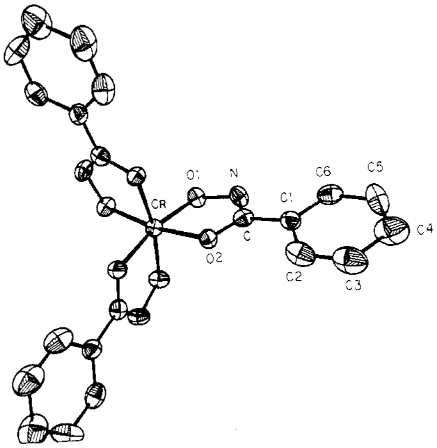

Figure 2. Perspective drawing of the *cis*-[Cr(benz-H)$_3$]$^{3-}$ anion, as viewed down the crystal and molecular threefold axis.

Description of Structures

cis-**[Cr(benz-H)$_3$]$^{3-}$.** The crystal structure consists of tris(benzohydroximato)chromate(III), sodium and iodide ions, and water, methanol, and ethanol molecules of crystallization as shown in Figure 1. The chromium atom lies at position (c) with C_3 site symmetry. The iodide ion lies on the other threefold axis at position (d). There is one sodium on the general position, one on position (b) with S_6 symmetry, and another on position (f) with C_2 symmetry. The sodium ions that lie on special positions along the 00*z* axis are coordinated by oxygen atoms of the hydroximate rings, while the other sodium ions are coordinated by water and methanol molecules. The oxygen atom that bridges sodium ions 1 and 3 (W3) (and forms relatively short coordinate bonds to both ions) is assigned as the hydroxide ion.

The structure of the *cis*-[Cr(benz-H)$_3$]$^{3-}$ anion and the atom-numbering scheme used are shown in Figure 2. Bond lengths and angles of the *cis*-[Cr(benz-H)$_3$]$^{3-}$ anion are given in Table IV. The hydroximate rings are planar and bend away from the chromium atom such that the average Cr-to-plane distance is 0.082 Å, and the dihedral angle between planes is 83.6° (Table V[23]). All sodium ions in the cis isomer have coordination numbers of 6 and are approximately octahedral. Bond lengths and angles of the coordination of sodium ions are given in Table VI.[23]

trans-**[Cr(benz-H)$_3$]$^{3-}$.** The crystal structure consists of the tris(benzohydroximato)chromate(III) anion, sodium ions, and

---

(19) Definitions of the indicators are $R = (\sum||F_o| - |F_c||)/\sum|F_o|$ and $R_w = [(\sum w(|F_o| - |F_c|)^2)/\sum wF_o^2 1^{1/2}$ and the error in an observation of unit weight is $[(\sum w(|F_o| - |F_c|)^2)/(N_o - N_v)]^{1/2}$, where N_o is the number of observations and N_v is the number of variables.

(20) Cromer, D. T.; Mann, B. *Acta Crystallogr., Sect. A* **1968**, *24*, 321–4.

(21) Stewart, R. F.; Davidson, E. T.; Simpson, W. T. *J. Chem. Phys.* **1965**, *42*, 3175–87.

(22) Cromer, D. T. *Acta Crystallogr.* **1965**, *18*, 17–23.

(23) Supplementary material.

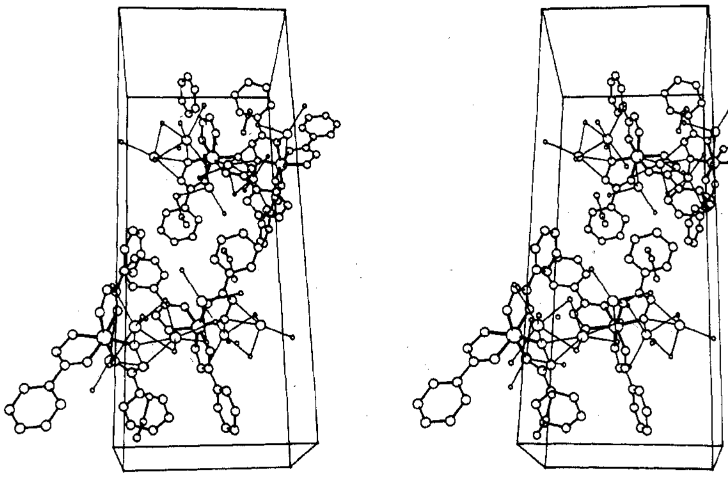

Figure 3. Stereoscopic packing diagram of the compound *trans*-$Na_3[Cr(PhC(O){=}N(O))_3]\cdot 8H_2O\cdot C_2H_5OH$. The structure is viewed down the *a* axis. The vertical axis is *c*.

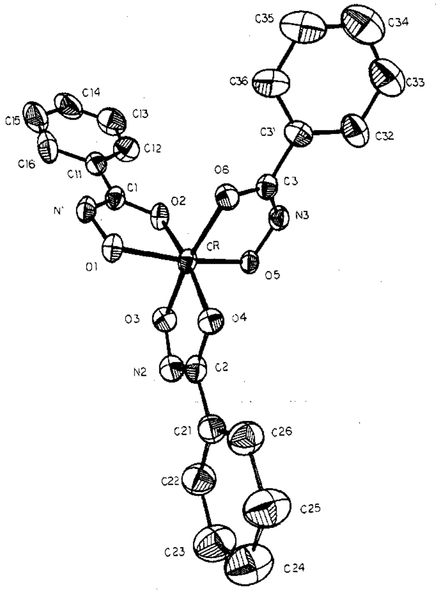

Figure 4. Perspective drawing of the *trans*-$[Cr(benz\text{-}H)_3]^{3-}$ anion, as viewed down the coordination threefold axis.

water and ethanol molecules of crystallization, as shown in Figure 3. The structure of the $[Cr(benz\text{-}H)_3]^{3-}$ anion and the atom-numbering scheme are shown in Figure 4. The chelate rings are arranged such that chelate ring 1 is in a trans relationship to chelate rings 2 and 3, with the chromium atom coordinated by six oxygen atoms in a trigonally distorted octahedral array. Bond lengths and angles involving the $[Cr(benz\text{-}H)_3]^{3-}$ anion are given in Table IV. The hydroximate chelate ring are planar and bend away from the chromium atoms such that the Cr-to-plane distances are 0.14, 0.04, and 0.41 Å for chelate rings 1, 2, and 3, respectively. The dihedral angles between planes range from 72.3 to 84.2°, as shown in Table V.[23] The sodium ions are coordinated by water molecules and by oxygen and nitrogen atoms of the hydroximate chelate rings. Sodium ion 3 is coordinated by six oxygen atoms in an approximate octahedral geometry, and sodium ion 1 has a coordination number of 5 with a distorted trigonal-pyramidal geometry. Sodium ion 2 is coordinated by five water molecules and the oxygen and nitrogen atoms of a hydroximate chelate ring in a distorted octahedral arrangement, with the oxygen and nitrogen atoms occupying the sixth position, where the oxygen–sodium–nitrogen angle is 33.8 (1)°. Bond lengths and angles of the coordination of the sodium ions are given in Table VI.[23]

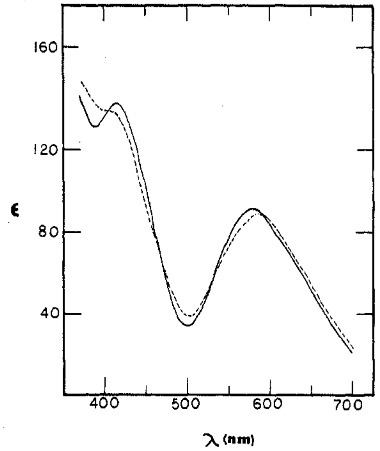

Figure 5. Visible absorption spectra of *cis*-$[Cr(benz\text{-}H)_3]^{3-}$ (—) and *trans*-$[Cr(benz\text{-}H)_3]^{3-}$ (- - -) in 2 M NaOH solution.

The average Cr–(*N*-hydroxyl oxygen) and Cr–(carbonyl oxygen) bond distances in *trans*-$[Cr(benz\text{-}H)_3]^{3-}$ are 1.955 (13) and 1.987 (12) Å, respectively; these bond distances compare well with those of the corresponding bonds in *trans*-$Cr(benz)_3$[12] [1.960 (4) and 1.984 (5) Å]. The moderately high esd's for the *trans*-$[Cr(benz\text{-}H)_3]^{3-}$ complex are due to the difference in Cr–O bond distances between the two cis and trans chelate rings as shown in Table IV. This difference reflects a tendency of the structure to approach a more symmetric structure which is in turn attributed to the crystal-field stabilization of the pure octahedral geometry for the d^3 chromic complex. The Cr–O bond distances are 1.951 (4) and 1.965 (2) Å for the *cis*-$[Cr(benz\text{-}H)_3]^{3-}$ isomer. These Cr–O bond distances in $[Cr(benz\text{-}H)_3]^{3-}$ complexes compare well with those found in $Cr(acac)_3$ [1.951 (6) Å],[24] *fac*-$Cr(gly)_3$ [1.965 (2) Å],[25] and $[Cr(oxl)_3]^{3-}$ [1.96 (4) Å][26] and are smaller than that found in $[Cr(catec)_3]^{3-}$ [1.986 (4) Å][27] (gly = glycenato, oxl = oxalato, and catec = catecholato).

Discussion

The visible absorption spectra of the *cis*- and *trans*-$[Cr(benz\text{-}H)_3]^{3-}$ complexes are shown in Figure 5. The spectra

---

(24) Morison, B. *Acta Crystallogr.* **1965**, *19*, 131–7.
(25) Bryan, R. F.; Greene, P. T.; Stokely, P. F.; Wilson, E. W., Jr. *Inorg. Chem.* **1971**, *10*, 1468–73.
(26) Van Niekerk, N. N.; Shöening, F. R. L. *Acta Crystallogr.* **1952**, *5*, 499–505.
(27) Raymond, K. N.; Isied, S. S.; Brown, L. D.; Fronczek, F. R.; Nibert, J. H. *J. Am. Chem. Soc.* **1976**, *98*, 1767–74.

Table II

A. Positional and Thermal Parameters (×10⁴) for the Nonhydrogen Atoms in *cis*-$Na_3Cr(benz\text{-}H)_3 \cdot NaI \cdot NaOH \cdot 9H_2O \cdot 3CH_3OH \cdot C_2H_5OH$

	x	y	z	β_{11}[a]	β_{22}	β_{33}	β_{12}	β_{13}	β_{23}
I	$^1/_3$	$^2/_3$	0.36500 (2)	62.0 (3)	β_{11}	9.92 (8)	$^1/_2\beta_{11}$	0	0
Cr	0	0	0.38457 (3)	36.9 (4)	β_{11}	4.1 (1)	$^1/_2\beta_{11}$	0	0
Na_1	−0.1989 (2)	0.1429 (2)	0.25206 (7)	65 (1)	53 (1)	11.8 (3)	30 (1)	2.1 (5)	1.8 (5)
Na_2	0	0	$^1/_2$	60 (3)	β_{11}	5.5 (5)	$^1/_2\beta_{11}$	0	0
Na_3	0.4213 (2)	0	$^1/_4$	69 (2)	60 (2)	12.7 (4)	$^1/_2\beta_{22}$	2.1 (4)	$2\beta_{13}$
O_1	0.0415 (3)	0.1356 (2)	0.3450 (1)	58 (2)	44 (2)	6.0 (3)	26 (2)	3.6 (7)	2.3 (7)
O_2	−0.0656 (2)	0.0672 (2)	0.42919 (9)	48 (2)	40 (2)	5.9 (3)	24 (2)	3.4 (7)	1.1 (7)
$O(CH_3OH)$	−0.2569 (3)	0.0030 (3)	0.1852 (1)	50 (2)	56 (3)	12.0 (5)	23 (2)	0 (9)	−1.0 (9)
O(W1)	0.1845 (3)	0	$^1/_4$	67 (3)	66 (4)	5.0 (5)	$^1/_2\beta_{22}$	2.8 (5)	$2\beta_{13}$
O(W2)	−0.1192 (3)	0.2862 (3)	0.1866 (1)	66 (3)	65 (3)	11.0 (5)	41 (2)	1.8 (9)	1.7 (9)
O(W3)	−0.1426 (3)	0.2886 (4)	0.3113 (1)	94 (4)	91 (4)	11.8 (6)	31 (3)	−2 (1)	0 (1)
O(W4)	−0.3712 (3)	0.1554 (3)	0.2479 (1)	49 (3)	96 (4)	17.0 (6)	33 (3)	0 (1)	8 (1)
N	0.0087 (3)	0.2086 (3)	0.3694 (1)	58 (3)	36 (2)	6.7 (4)	20 (2)	2.5 (9)	−1.4 (8)
$O(C_2H_5OH)$	$^1/_3$	$^2/_3$	0.1861 (3)	97 (4)	β_{11}	15 (1)	$2\beta_{11}$	0	0
$C_1(C_2H_5OH)$	$^1/_3$	$^2/_3$	0.1414 (4)	57 (4)	β_{11}	16 (1)	$2\beta_{11}$	0	0
C	−0.0433 (3)	0.1654 (3)	0.4123 (1)	42 (3)	41 (3)	6.4 (5)	21 (2)	−1.9 (9)	−0.3 (9)
C_1	−0.0836 (3)	0.2290 (3)	0.4428 (2)	49 (3)	41 (3)	8.7 (5)	23 (3)	−4 (1)	−5 (1)
C_2	−0.1544 (4)	0.1751 (4)	0.4837 (2)	63 (4)	63 (4)	13.1 (7)	36 (3)	11 (1)	−1 (1)
C_3	−0.1937 (5)	0.2311 (5)	0.5141 (2)	83 (5)	88 (5)	18 (1)	54 (4)	11 (2)	−2 (2)
C_4	−0.1643 (5)	0.3395 (5)	0.5030 (3)	99 (6)	85 (5)	21 (1)	56 (5)	14 (2)	−7 (2)
C_5	−0.0962 (5)	0.3938 (4)	0.4622 (2)	103 (5)	55 (4)	17.7 (9)	54 (4)	−4 (2)	−3 (2)
C_6	−0.0540 (4)	0.3399 (4)	0.4322 (2)	74 (4)	51 (3)	9.9 (6)	35 (3)	1 (1)	−2 (1)
$C(CH_3OH)$	−0.3248 (6)	0.0005 (6)	0.1438 (2)	103 (6)	107 (6)	15.2 (9)	63 (5)	−11 (2)	−3 (2)

B. Positional and Thermal Parameters (×10⁴) for the Nonhydrogen Atoms in *trans*-$Na_3Cr(benz\text{-}H)_3 \cdot 8H_2O \cdot C_2H_5OH$

Cr	0.97021 (4)	0.94365 (4)	0.78354 (1)	39.6 (3)	31.8 (3)	9.52 (6)	1.7 (3)	0.6 (1)	0.0 (1)
Na_1	0.0948 (1)	0.5510 (1)	0.29655 (4)	71 (1)	70 (1)	14.1 (2)	10.4 (9)	3.8 (4)	4.4 (4)
Na_2	1.0194 (1)	0.3071 (1)	0.79098 (4)	70 (1)	45.0 (9)	14.0 (2)	2.9 (8)	−0.8 (3)	2.9 (3)
Na_3	0.7543 (1)	0.3898 (1)	0.29346 (5)	67 (1)	76 (1)	18.2 (2)	−7 (1)	9.7 (4)	−7.2 (4)
O_1	0.9153 (2)	0.7767 (2)	0.77101 (6)	56 (2)	39 (1)	9.9 (3)	0.0 (1)	−1.2 (5)	0.6 (5)
O_2	1.0498 (2)	0.8678 (2)	0.84009 (7)	63 (2)	40 (1)	11.2 (3)	−5 (1)	−5.6 (6)	0.7 (5)
O_3	1.1262 (2)	0.9287 (2)	0.74928 (7)	46 (2)	59 (2)	11.5 (3)	13 (1)	3.1 (5)	3.0 (6)
O_4	0.9020 (2)	1.0027 (2)	0.72086 (6)	45 (2)	50 (2)	9.8 (3)	11 (1)	3.2 (5)	0.6 (5)
O_5	1.0273 (2)	0.0992 (2)	0.80626 (7)	51 (2)	38 (1)	11.6 (3)	−3 (1)	4.8 (5)	−0.5 (5)
O_6	0.6852 (2)	0.4889 (2)	0.68203 (6)	51 (2)	47 (1)	10.3 (3)	7 (1)	3.3 (5)	2.4 (5)
O(W1)	0.5376 (2)	0.1561 (2)	0.15237 (9)	105 (3)	87 (2)	21.3 (5)	8 (2)	10.5 (9)	−1.0 (8)
O(W2)	0.8680 (2)	0.4711 (2)	0.78583 (7)	81 (2)	42 (2)	14.8 (3)	2 (2)	−0.9 (7)	−7.1 (6)
O(W3)	0.8507 (2)	0.2537 (2)	0.73241 (8)	58 (2)	41 (2)	17.2 (3)	5 (1)	−2.1 (6)	−4.6 (6)
O(W4)	1.0032 (2)	0.6492 (2)	0.69839 (8)	97 (2)	85 (2)	13.4 (3)	−7 (2)	6.4 (7)	−5.7 (7)
O(W5)	0.8745 (3)	0.4949 (3)	0.2283 (2)	120 (3)	132 (4)	46.9 (9)	18 (3)	16 (1)	23 (2)
O(W6)	0.7313 (2)	0.0066 (2)	0.13305 (8)	65 (2)	76 (2)	16.9 (4)	−8 (2)	−0.5 (7)	0.5 (7)
O(W7)	0.3049 (3)	0.7553 (2)	0.76448 (9)	150 (3)	127 (3)	14.7 (4)	75 (3)	−0.5 (9)	−5.5 (8)
O(W8)	0.7253 (2)	0.2023 (2)	0.33906 (8)	122 (3)	102 (2)	12.9 (3)	63 (2)	5.4 (8)	0.7 (7)
O(Eth)	0.6339 (2)	0.3243 (2)	0.41571 (8)	120 (3)	117 (3)	11.0 (3)	19 (2)	−0.4 (7)	0.2 (7)
N_1	0.9511 (2)	0.7000 (2)	0.80922 (8)	63 (2)	36 (2)	10.1 (3)	−2 (2)	0.4 (7)	0.9 (6)
N_2	1.1091 (2)	0.9608 (2)	0.70140 (8)	51 (2)	57 (2)	11.9 (3)	12 (2)	4.8 (6)	1.6 (7)
N_3	0.4516 (2)	0.3584 (2)	0.34263 (8)	65 (2)	41 (2)	11.3 (3)	3 (2)	3.4 (7)	2.0 (6)
C_1	1.0178 (2)	0.7543 (2)	0.84244 (9)	50 (2)	38 (2)	10.6 (4)	1 (2)	2.4 (8)	1.3 (7)
C_{11}	0.9411 (3)	0.3118 (3)	0.1140 (1)	61 (3)	56 (2)	11.4 (4)	7 (2)	4.1 (8)	3.3 (8)
C_{12}	0.8899 (4)	0.2496 (3)	0.0754 (1)	124 (4)	83 (3)	11.4 (5)	0 (3)	−3 (1)	0 (1)
C_{13}	0.8539 (4)	0.3078 (4)	0.0341 (1)	146 (5)	141 (5)	11.5 (5)	1 (4)	−3 (1)	4 (1)
C_{14}	0.8701 (4)	0.4307 (4)	0.0313 (1)	126 (4)	140 (5)	13.9 (6)	25 (4)	7 (1)	23 (1)
C_{15}	0.9185 (4)	0.4926 (4)	0.0688 (1)	163 (5)	86 (4)	17.0 (6)	4 (4)	3 (2)	17 (1)
C_{16}	0.09562 (4)	0.4345 (3)	0.1104 (1)	132 (4)	59 (3)	15.0 (5)	0 (3)	−1 (1)	8 (1)
C_2	0.4927 (2)	0.5016 (2)	0.19043 (9)	53 (2)	38 (2)	10.3 (4)	0 (2)	3.8 (8)	0.7 (7)
C_{21}	0.4618 (3)	0.4581 (2)	0.1422 (1)	69 (3)	54 (2)	9.5 (4)	−1 (2)	4.6 (8)	−0.3 (8)
C_{22}	0.3372 (3)	0.4178 (3)	0.1288 (1)	80 (3)	94 (3)	10.5 (4)	−10 (3)	6.1 (9)	−6.2 (9)
C_{23}	0.3069 (4)	0.3777 (4)	0.0837 (1)	96 (4)	136 (4)	13.6 (5)	−24 (3)	1 (1)	−13 (1)
C_{24}	0.3992 (4)	0.37771 (4)	0.0512 (1)	133 (5)	146 (5)	11.0 (5)	−7 (4)	7 (1)	−15 (1)
C_{25}	0.5237 (4)	0.4143 (4)	0.0642 (1)	112 (4)	147 (5)	12.9 (5)	−3 (4)	15 (1)	−11 (1)
C_{26}	0.5550 (3)	0.4539 (3)	0.1093 (1)	83 (3)	96 (3)	14.3 (5)	−7 (3)	10 (1)	−6 (1)
C_3	0.3448 (2)	0.4193 (2)	0.34509 (9)	55 (2)	44 (2)	9.2 (4)	−4 (2)	−0.2 (7)	−0.6 (7)
C_{31}	0.2536 (3)	0.3822 (3)	0.3799 (1)	61 (3)	76 (3)	8.9 (4)	−2 (2)	0.3 (8)	3.7 (8)
C_{32}	0.1815 (3)	0.4685 (3)	0.4014 (1)	100 (4)	101 (4)	11.0 (4)	7 (3)	8 (1)	1 (1)
C_{33}	0.0897 (4)	0.4336 (5)	0.4327 (1)	120 (4)	168 (6)	15.3 (6)	24 (4)	19 (1)	3 (2)
C_{34}	0.0721 (4)	0.3155 (5)	0.4430 (2)	137 (5)	182 (6)	16.5 (7)	−23 (5)	20 (2)	16 (2)
C_{35}	0.1444 (4)	0.2304 (4)	0.4226 (1)	141 (5)	125 (4)	16.4 (6)	−43 (4)	8 (1)	15 (1)
C_{36}	0.2351 (3)	0.2620 (3)	0.3909 (1)	108 (4)	80 (3)	12.9 (5)	−17 (3)	5 (1)	6 (1)
Cl(Eth)	0.5815 (6)	0.3544 (6)	0.4584 (2)	222 (8)	278 (9)	11.4 (6)	−67 (7)	9 (2)	−19 (2)
C2(Eth)	0.6691 (8)	0.3783 (9)	0.4938 (3)	441 (15)	718 (22)	41 (1)	−41 (14)	−4 (4)	−27 (5)

[a] The form of the anisotropic thermal ellipsoid is $\exp[-(\beta_{11}h^2 + \beta_{22}k^2 + \beta_{33}l^2 + 2\beta_{12}hk + 2\beta_{13}hl + 2\beta_{23}kl)]$.

Table IV. Bond Distances (Å) and Angles (Deg) for the $[Cr(benz\text{-}H)_3]^{3-}$ Complexes

	trans-$[Cr(benz\text{-}H)_3]^{3-}$				
bond dist or angle	ring 1	ring 2	ring 3	av[b]	*cis*-$[Cr(benz\text{-}H)_3]^{3-}$
$Cr\text{-}O_n$	1.981 (2)	1.944 (2)	1.939 (2)	1.955 (13)	1.956 (2)
$Cr\text{-}O_m$	1.962 (2)	1.998 (2)	2.000 (2)	1.987 (12)	1.968 (2)
$O_n\text{-}N$	1.422 (3)	1.418 (3)	1.422 (3)	1.421 (3)	1.443 (4)
$O_m\text{-}C$	1.317 (3)	1.319 (3)	1.314 (3)	1.317 (3)	1.308 (4)
C-N	1.294 (3)	1.305 (3)	1.305 (3)	1.301 (4)	1.298 (4)
$C\text{-}C_1$	1.491 (4)	1.486 (4)	1.480 (4)	1.486 (4)	1.481 (5)
$C_1\text{-}C_2$	1.397 (4)	1.400 (4)	1.406 (5)	1.401 (5)	1.387 (5)
$C_2\text{-}C_3$	1.377 (5)	1.378 (5)	1.401 (6)	1.385 (8)	1.400 (6)
$C_3\text{-}C_4$	1.400 (7)	1.393 (6)	1.400 (8)	1.398 (8)	1.362 (7)
$C_4\text{-}C_5$	1.379 (6)	1.372 (6)	1.383 (7)	1.378 (7)	1.391 (7)
$C_5\text{-}C_6$	1.395 (5)	1.402 (5)	1.394 (6)	1.394 (6)	1.393 (6)
$C_6\text{-}C_1$	1.402 (4)	1.400 (4)	1.405 (5)	1.402 (5)	1.400 (5)
$O_n\text{-}Cr\text{-}O_m$	80.78 (8)	80.24 (7)	80.91 (7)	80.6 (2)	81.5 (1)
$Cr\text{-}O_n\text{-}N$	112.0 (1)	114.2 (1)	112.2 (1)	112.8 (9)	112.2 (2)
$Cr\text{-}O_m\text{-}C$	111.6 (2)	111.0 (1)	108.9 (2)	110.5 (8)	111.2 (2)
$O_n\text{-}N\text{-}C$	112.6 (2)	112.2 (2)	111.6 (2)	112.1 (3)	111.6 (3)
$O_m\text{-}C\text{-}N$	122.8 (2)	122.6 (2)	123.3 (2)	122.9 (2)	123.4 (3)
$O_m\text{-}C\text{-}C$	118.0 (2)	119.2 (2)	117.6 (2)	118.3 (5)	117.3 (3)
N-C-C	119.1 (2)	118.2 (2)	119.1 (2)	118.8 (3)	119.2 (3)
phenyl C-C-C				120.0 (2)	120.0 (2)

[a] Atom numbers correspond to those in Figure 2. [b] Averages are computed as $\bar{x} = (1/n)\Sigma x_i$ and $\sigma^2(\bar{x}) = [1/[n(n-1)]][\Sigma(x_i - x)^2]$.

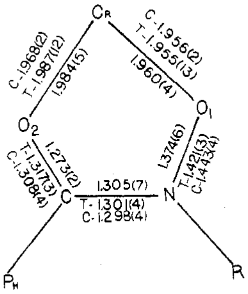

Figure 6. Comparison of the average bond lengths (Å) of the chelate rings in neutral *trans*-tris(benzohydroxamato)chromium(III) (R = H; bond lengths inside the chelate ring) and *cis*- and *trans*-tris(benzohydroximato)chromate(III) trianions (R = two electrons; bond lengths outside the chelate ring; C = cis; T = trans).

Table VII. Comparison of Structural Parameters for *trans*-$Cr(benz)_3$ and *trans*- and *cis*-$[Cr(benz\text{-}H)_3]^{3-}$

bond dist or angle[a,d]	*trans*-Cr-$(benz)_3$[b]	*trans*-[Cr-$(benz\text{-}H)_3]^{3-}$	*cis*-[Cr-$(benz\text{-}H)_3]^{3-}$
$Cr\text{-}O_1$	1.960 (4)	1.955 (13)	1.956 (2)
$Cr\text{-}O_2$	1.984 (5)	1.987 (12)	1.968 (2)
$O_1\text{-}N$	1.374 (6)	1.421 (3)	1.443 (4)
$O_2\text{-}C$	1.273 (2)	1.317 (3)	1.308 (4)
C-N	1.305 (7)	1.301 (4)	1.298 (4)
$O_1\text{-}Cr\text{-}O_2$	81.0 (2)	80.6 (2)	81.5 (1)
$Cr\text{-}O_1\text{-}N$	109.4 (6)	112.8 (9)	112.2 (2)
$Cr\text{-}O_2\text{-}C$	112.0 (2)	110.5 (8)	111.2 (2)
$O_1\text{-}N\text{-}C$	117.8 (5)	112.1 (3)	111.6 (3)
$O_2\text{-}C\text{-}N$	118.8 (4)	122.9 (2)	123.4 (3)
$O_2\text{-}C\text{-}C_1$	120.6 (4)	118.3 (5)	117.3 (3)
$N\text{-}C\text{-}C_1$	120.6 (3)	119.8 (3)	119.2 (3)
$O_1\text{-}O_2$	2.561 (2)	2.551 (5)	2.561 (3)
ligand bite (b)	1.36	1.29	1.31
trigonal twist angle (ϕ)	47.4 (1)	49.9 (9)	47.1 (1)
calcd twist angle[c]	48.2	47.5	48.4

[a] Atom numbers correspond to those of Figure 2. [b] Reference 12. [c] Using the relation $\phi = -73.9 + 94.10b$.[26] [d] Bond distances in angstroms and bond angles in degrees.

parallel those of the corresponding neutral *cis*- and *trans*-$Cr(benz)_3$ complexes;[11,12] the cis isomer absorbs at higher and lower energy for the spin-allowed d–d transitions, $^4A_{2g} \rightarrow {}^4T_{2g}$ and $^4A_{2g} \rightarrow {}^4T_{1g}$, respectively. The shift of ~9–14 nm toward higher energy for the $^4A_{2g} \rightarrow {}^4T_{2g}$ transition in the spectra of both isomers upon deprotonation reflects an increase in the ligand field caused by the greater charge on the coordinating oxygen atoms.

The *cis*- and *trans*-$[Cr(benz\text{-}H)_3]^{3-}$ isomers are obtained from the neutral hydroxamato complexes of *opposite* geometries. The isomerization process accompanying the deprotonation of the hydroxamato complexes effects a complete conversion in geometry—a process which is not understood as yet. Both *cis*- and *trans*-$[Cr(benz\text{-}H)_3]^{3-}$ isomers isomerize rapidly in aqueous solution in the pH range 9–12 but are more stable in strongly basic solutions ($[OH^-] > 2$ M).

Bonding in Hydroxamato and Hydroximato Complexes. A comparison between bond distances and bond angles of the hydroxamato chelate ring in *trans*-$Cr(benz)_3$ and the hydroximato chelate rings in *cis*- and *trans*-$[Cr(benz\text{-}H)_3]^{3-}$ complexes is given in Table VII and Figure 6. The main changes upon deprotonation of the hydroxamato complex are an increase in the N–O and C–O bond distances of 0.05 and 0.04 Å, respectively. This is accompanied by only a small change in the C–N bond. The O–C–N bond angle increases by ~4°, and the O–N–C bond angle decreases by 7° upon deprotonation, a stereochemical effect of the lone pair on the nitrogen which results from deprotonation. The average C–O bond distances of 1.273 (2) Å in $Cr(benz)_3$ and 1.308 (4) and 1.317 (3) Å in *cis*- and *trans*-$[Cr(benz\text{-}H)_3]^{3-}$ complexes, respectively, are longer than the C–O bond found in simple carbonyl compounds (1.23 Å),[28] and the C–O bonds in the hydroximato complexes are slightly longer than the distances found in zwitterionic compounds such as DL-serine, 1.26 Å.[28] The C–N bond distances in both the hydroximato and hydroxamato complexes (~1.30 Å) are significantly shorter than C–N single bonds (1.43–1.45 Å[28]) and are only slightly longer than the C=N bond found in ethylbenzohydroximic acid (PhC(OEt)=N(OH) = 1.27 Å).[29] In contrast to the thiohydroxamate complex for which both Cr–O and Cr–S bond distances increase upon deprotonation, only a slight change is observed in the Cr–O bond distances upon deprotonating the *trans*-$Cr(benz)_3$ complex—a slight increase and decrease in the Cr–O(carbonyl) and Cr–O(*N*-hydroxyl) bonds, respectively. These bond distances can be interpreted by reso-

---

(28) Oosthock, V. A. N. "Molecular Structure and Dimensions"; Kennard, O., Watson, D. G., Allen, F. H., Isaacs, N. W., Motherwell, W. D., Pattersen, R. C., Town, W. G., Eds.; Vitegevefs Mij: Utrecht, 1972.

(29) Larsen, I. K. *Acta. Chem. Scand.* **1971**, *25*, 2408–09.

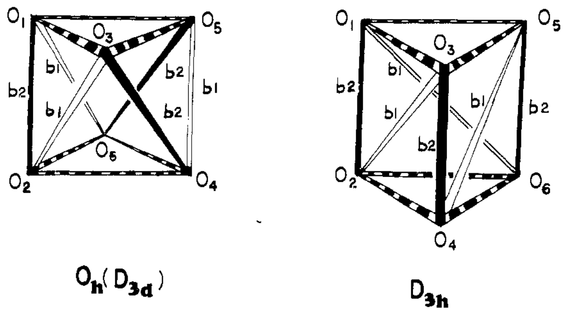

Figure 7. Six-atom family shape characteristics (see text).

nance structures Ia,b and IIa,b for the hydroxamato and hydroximato metal complexes.

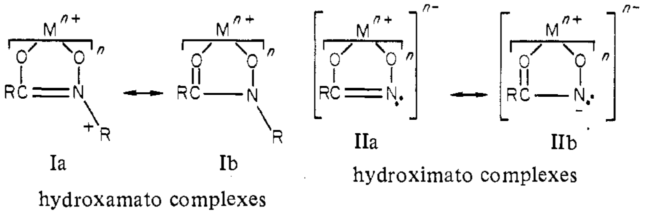

From the bond lengths observed in these structures (particularly C⎓N) it can be seen that the forms Ia and IIa dominate the electronic structure of the ligand. Futhermore, structure IIb is highly implausible because of the charge localization in the NO group compared to IIa. The fact that the C–N bond order does not change substantially in the hydroxamate ↔ hydroximate interconversion is then also consistent with Ia being more important than Ib in the electronic structure of the hydroxamate ligand.

Coordination Geometries. Two theoretical models have been presented for the detailed analysis of tris-chelate geometries,[30,31] but both reach substantially the same conclusion. It was found that the twist angle (ϕ, the average of the projection angles of the top and bottom triangular faces perpendicular to the C_3 or pseudo-C_3 axis) is a linear function of the ligand bite (b, ratio of ring O–O distance to M–O distance) for a wide range of tris-chelate complexes. An empirical relation between ϕ and b has been presented: $\phi = -73.9 + 94.10b$.[29] Observed and calculated twist angles and other parameters for *trans*-Cr(benz)$_3$ and *cis*- and *trans*-[Cr(benz-H)$_3$]$^{3-}$ are compared in Table VII. Although the hydroxamate complexes were not used in obtaining the above equation, the calculated twist angles are in agreement with those observed.

An alternative description of how close the coordination geometry is to either the trigonally elongated octahedral (trigonal antiprism, D_{3d}) or the trigonal-prismatic (D_{3h}) geometry is through so-called shape parameters—the dihedral angles between trigonal faces sharing common edges of the polyhedron.[32,33] The ideal and observed dihedral angles for *trans*-Cr(benz)$_3$ and *cis*- and *trans*-[Cr(benz-H)$_3$]$^{3-}$ (corresponding to Figure 7) are shown in Table VIII. It is clear from the data presented that both twist angle and dihedral angle treatments place these chromic hydroxamato and hydroximato complexes in the same position along the D_{3d}–D_{3h} reaction path, close to the trigonal-antiprismatic (D_{3d}) geometry. *trans*-Cr(benz)$_3$ and *trans*-[Cr(benz-H)$_3$]$^{3-}$ show a close similarity in the overall geometry of the coordination octahedra. This similarity and the very similar spectroscopic properties of the hydroxamate and hydroximate complexes mean that the stereochemical assignments of the hydroximate anion complexes (based on spectra) can be carried over to the neutral hydroxamate complexes, including the hydroxamate siderophores.

Table VIII. Ideal and Observed Dihedral Angles (Deg) for *trans*-Cr(benz)$_3$ and *trans*- and *cis*-[Cr(benz-H)$_3$]$^{3-}$ Complexes[a]

complex	δ's at b_1	δ's at b_2	remaining δ's
ideal octahedron	70.5, 70.5, 70.5	70.5, 70.5, 70.5	70.5, 70.5, 70.5 70.7, 70.5, 70.5
ideal trigonal prism	0, 0, 0	120, 120, 120	90, 90, 90 90, 90, 90
trans-Cr(benz)$_3$	60.5, 62.3, 65.7	79.2, 79.9, 82.9	67.4, 66.6, 68.9 69.3, 71.7, 72.4
trans-[Cr(benz-H)$_3$]$^{3-}$	62.3, 63.6, 65.7	79.4, 80.1, 80.5	66.6, 67.4, 68.9 69.3, 71.7, 72.4
cis-[Cr(benz-H)$_3$]$^{3-}$	60.1, 60.1, 60.1	81.4, 81.4, 81.4	69.4, 69.4, 69.4 72.0, 72.0, 72.0

[a] See Figure 7.

Summary

The cis and trans isomers of the anionic tris(hydroximato)chromate(III) complex have been isolated and structurally characterized. Interconversion of the neutral hydroxamate and anionic hydroximate complexes occurs via loss of a proton on the hydroxamate nitrogen. This results in only small changes in bond lengths within either the CrO_6 coordination polyhedron or the ligand. The cis and trans hydroximate complexes also have very similar geometries. These results support a view of these complexes as rigid, octahedral complexes in which the hydroxmate ligand has substantial negative charge on both oxygen atoms and nearly full formation of a C=N double bond in the center of the ring.

Acknowledgment. The structural aspects of this research are supported by the National Science Foundation. Support for the microbial iron transport project is provided by the NIH (Grant AI 11744). The authors wish to acknowledge the assistance of Dr. D. P. Freyberg and Mr. W. Smith.

Registry No. $Na_3Cr(benz\text{-}H)_3 \cdot NaI \cdot 9H_2O \cdot 3CH_3OH \cdot C_2H_5OH \cdot NaOH$, 73209-44-6; $Na_3Cr(benz\text{-}H)_3 \cdot 8H_2O \cdot C_2H_5OH$, 73178-82-2; *trans*-tris(benzohydroxamato)chromium(III), 52194-27-1; *cis*-tris(benzohydroxamato)chromium(III), 52304-90-2.

Supplementary Material Available: Table III, root-mean-square amplitudes of vibrations along principal axes; Table V, weighted least-squares planes and dihedral angles; Table VI, bond distance and angle data; a listing of structure factor amplitudes (55 pages). Ordering information is given on any current masthead page.

---

(30) Kepert, D. L. *Inorg. Chem.* **1972**, *11*, 1561–3.
(31) Avdeef, A.; Fackler, J. P., Jr. *Inorg. Chem.* **1975**, *14*, 2002–6.
(32) Porai-Koshits, M. A.; Aslanov, L. A. *Zh. Strukt. Khim.* **1972**, *13*, 266–76.
(33) Muetterties, E. L.; Guggenberger, L. J. *J. Am. Chem. Soc.* **1974**, *96*, 1748–56.